# DESIGN AND OPTIMIZATION OF 2 GHz TRAVELING-WAVE STRUCTURES FOR THE CLIC MAIN BEAM INJECTOR LINACS

A. Kurtulus*, S. Doebert, A. Grudiev, A. Latina, Y. Zhao
CERN, Geneva, Switzerland

*Abstract*

The design of the CLIC main beam injector linacs requires high-gradient, traveling-wave accelerating structures capable of handling substantial beam-loading effects due to high beam currents. In this work, we present a comprehensive design and optimization study of 2 GHz traveling-wave structures for the electron and positron linacs, which accelerate beams up to 2.8 GeV with a nominal bunch charge of 1 nC, and the booster linac, reaching 9 GeV with a 0.83 nC bunch charge. Each bunch train consists of 352 bunches, necessitating careful management of beam dynamics and wakefield effects. Using analytical modeling and extensive parameter scans, we optimized the iris geometry to enhance shunt impedance, reduce surface electric fields, and suppress long-range wakefields through detuning strategies. Beam-loading effects were analyzed, and compensation techniques were implemented to minimize bunch-to-bunch energy spread, ensuring stable and efficient acceleration. This study advances the development of high-performance linac structures capable of operating with high beam currents, supporting the reliable achievement of CLIC performance goals.

## INTRODUCTION AND RF DESIGN METHODOLOGY

The CLIC 380 GeV baseline [1] requires a Main Beam Injector (MBI) complex delivering electrons and positrons to damping rings at 2.86 GeV and then to a booster linac reaching 9 GeV. The injector linacs operate at 2 GHz with bunch charges of 1 nC for the injectors and 0.83 nC for the booster, 352 bunches per train at 0.5 ns spacing, and a 100 Hz repetition rate [1]. The electron injector linac must accelerate two bunch trains per cycle: one for the main electron beam and one for positron-production electrons. The booster linac similarly accelerates two bunch trains: positrons and electrons. The positron injector linac accelerates only one positron bunch train per cycle. These conditions demand high RF-to-beam efficiency, careful compensation of cumulative beam loading, and robust suppression of long-range transverse wakefields to preserve beam quality. A detailed description of the full RF design methodology and optimization framework is provided in our companion paper [2].

We adopt 3 m traveling-wave accelerating structures, aligned with FCC-ee injector development [3]. Each cell is defined by the aperture radius $a$, the iris thickness $d$, and the RF phase advance per cell $\psi$. An RF parameter database of over 200 geometries was compiled using CST eigenmode simulations at 5.712 GHz, then scaled to 2 GHz. For each geometry we extract the normalized shunt impedance $\rho$, the quality factor $Q$, the group velocity $v_g$, and the surface field quantities [4], namely the maximum surface electric field $E_{s,\max}$ and the maximum Poynting vector $S_{c,\max}$. The 20 lowest dipole higher-order modes are also computed for subsequent wakefield analysis.

To increase the voltage for given peak klystron RF power, a SLED RF pulse compressor is used [5]. The goal is to produce a high-gain, flat-top compressed RF pulse that maintains stable accelerating conditions throughout the beam pulse. The compressed pulse length $t_p$ is the sum of the bunch train duration (176 ns) and the RF structure filling time. Figure 1 shows the klystron drive amplitude and the resulting compressed RF pulse. For a given $t_p$, we determine the optimal SLED coupling coefficient $\beta$ and the resulting amplitude gain $A_{\text{gain}}$ (Fig. 2). The peak input power to the structure is then $P_{\text{in}} = P_k \cdot A_{\text{gain}}^2$, where $P_k = 80$ MW is the peak klystron power.

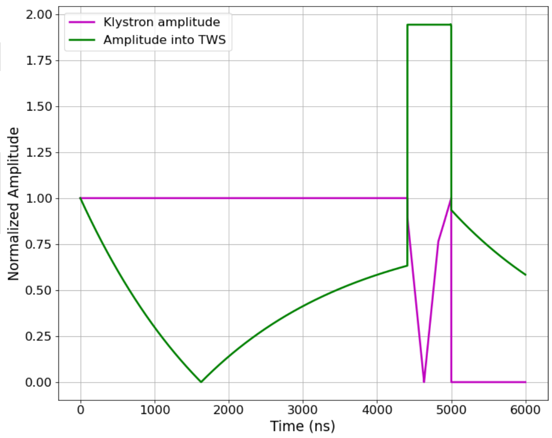


Figure 1: Klystron amplitude (magenta) and compressed RF pulse (green).

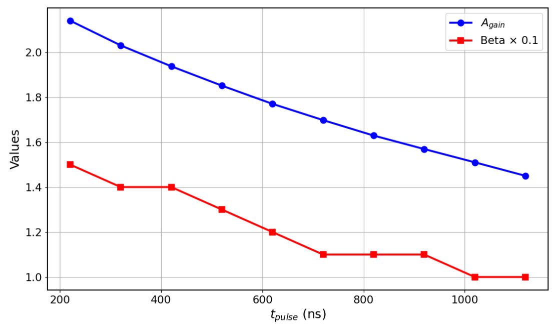


Figure 2: Amplitude gain $A_{\text{gain}}$ (blue) and coupling $\beta$ (red) vs $t_p$.

* adnan.kurtulus@cern.ch

For a given average aperture $\langle a \rangle$ set by beam dynamics requirements, we perform a 2D scan over the first-cell iris thickness $d_{\mathrm{first}}$ and last-cell iris thickness $d_{\mathrm{last}}$. Each combination defines a different tapered geometry. For each design, we compute the beam-loaded accelerating voltage $V_{\mathrm{L}}$ using the analytical traveling-wave formalism [6]. To suppress long-range transverse wakefields, we taper the aperture with parameter $\Delta$: $a_{\mathrm{first}} = \langle a \rangle + \Delta$, $a_{\mathrm{last}} = \langle a \rangle - \Delta$. This spreads dipole mode frequencies, preventing coherent wakefield buildup. The wakefield severity is quantified by $W_{\mathrm{t,tot}}$, the sum of absolute transverse wake potentials over all 352 trailing bunches. Beam dynamics stability requires $W_{\mathrm{t,tot}} < 10$ V/pC/mm/m [7]. Among designs satisfying this constraint, we select the one maximizing $V_{\mathrm{L}}$. Figure 3 shows an example for $\langle a \rangle = 18$ mm.

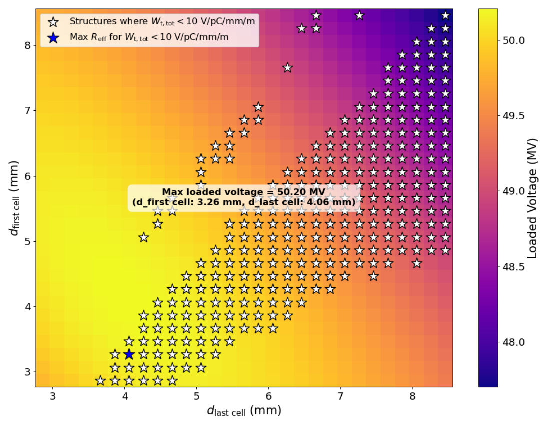


Figure 3: $V_{\mathrm{L}}$ for $\langle a \rangle = 18$ mm. White stars: $W_{\mathrm{t,tot}} < 10$; blue star: optimal.

## BOOSTER LINAC AND ELECTRON INJECTOR LINAC

The booster and electron injector linacs share the same structure but differ in bunch charge: 0.83 nC (booster) and 1.00 nC (electron injector). A scan over $\langle a \rangle = 12 - 19$ mm and $\Delta = 0 - 5$ mm identified the optimal configuration: $\langle a \rangle = 18$ mm, $\Delta = 3$ mm (Table 1).

Table 1: Baseline Structure ($\langle a \rangle = 18$ mm, $\Delta = 3$ mm).

| Parameter | Value | Unit |
|---|---|---|
| Frequency | 2 | GHz |
| Length | 3 | m |
| Avg. aperture | 18 | mm |
| Aperture (first/last) | 21/15 | mm |
| Iris thickness (first/last) | 3.26/4.06 | mm |
| $v_g/c$ (first/last) | 4.21/1.39 | % |
| $\rho$ (first/last) | 2.58/3.22 | kΩ/m |
| $Q$ (first/last) | 19799/19519 | – |
| Filling time | 416 | ns |
| $W_{\mathrm{t,tot}}$ | 9.15 | V/pC/mm/m |
| Klystron power | 31 | MW |

### *Single-train Operation*

Applying beam-loading compensation RF pulse shape yields flat accelerating gradients (Fig. 4). Achieved average loaded gradients: 18.47 MV/m (booster) and 17.67 MV/m (electron injector) (Table 2).

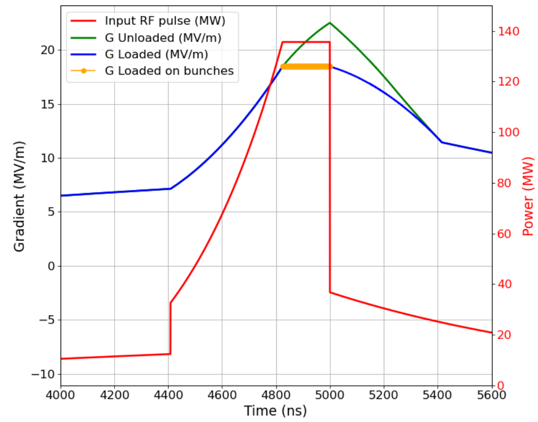


Figure 4: Unloaded (green) and beam-loaded (blue) gradients with compensation.

Table 2: Single-train Performance

| Parameter | Booster | e- Injector | Unit |
|---|---|---|---|
| Bunch charge | 0.83 | 1.00 | nC |
| $V_{\mathrm{L}}$ | 55.4 | 53 | MV |
| Avg. $G_{\mathrm{L}}$ | 18.47 | 17.67 | MV/m |
| $E_{s,\mathrm{max}}$ | 81 | 82 | MV/m |
| $S_{c,\mathrm{max}}$ | 494 | 509 | mW/μm$^2$ |

### *Double-train Operation*

To reduce average RF power, we accelerate two trains within a single compressed pulse. Achieved gradients: 13.52 MV/m (booster) and 12.73 MV/m (electron injector), with 0.1% energy spread. Wakefields remain within limits (9.15 and 7 V/pC/mm/m). The effective repetition rate drops from 200 to 100 Hz. Figure 5 and Table 3 summarize the results.

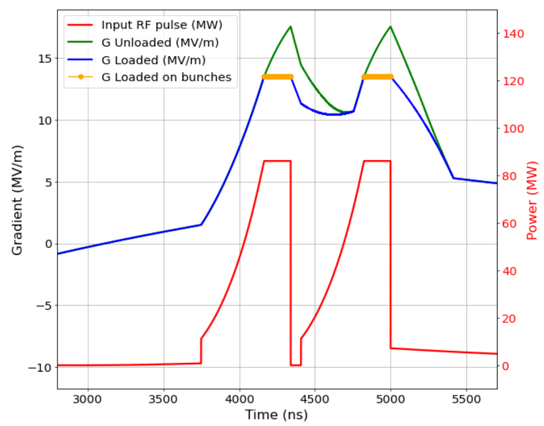


Figure 5: Gradients for Double-train Operation

Table 3: Double-train Performance

| Parameter | Booster | e- Injector | Unit |
|---|---|---|---|
| Bunch charge | 0.83 | 1.00 | nC |
| $V_\mathrm{L}$ | 40.55 | 38.18 | MV |
| Avg. $G_\mathrm{L}$ | 13.52 | 12.73 | MV/m |
| $E_{s,\mathrm{max}}$ | 64 | 66 | MV/m |
| $S_{c,\mathrm{max}}$ | 314 | 326 | mW/μm$^2$ |

## POSITRON INJECTOR LINAC

Due to larger emittance, the positron injector requires a larger aperture. The optimized structure has $\langle a \rangle = 22$ mm, $\Delta = 2$ mm, and 120° phase advance. Applying the same beam-loading compensation yields the final parameters in Table 4.

Table 4: Final Parameters for the Positron Injector

| Parameter | Value | Unit |
|---|---|---|
| Frequency | 2 | GHz |
| Length | 3 | m |
| Avg. aperture | 22 | mm |
| Aperture (first/last) | 24/20 | mm |
| Iris thickness (first/last) | 8.46/8.46 | mm |
| $v_g/c$ (first/last) | 4.44/2.50 | % |
| $\rho$ (first/last) | 2.21/2.57 | kΩ/m |
| $Q$ (first/last) | 18619/18490 | – |
| Filling time | 300 | ns |
| Klystron power | 31 | MW |
| Bunch charge | 1.00 | nC |
| $V_\mathrm{L}$ | 46.24 | MV |
| Avg. $G_\mathrm{L}$ | 15.41 | MV/m |
| $E_{s,\mathrm{max}}$ | 46 | MV/m |
| $S_{c,\mathrm{max}}$ | 240 | mW/μm$^2$ |
| $W_{\mathrm{t,tot}}$ | 10.13 | V/pC/mm/m |
| Energy spread | 0.01 | % |

## CONCLUSION

We have presented optimized 2 GHz traveling-wave structures for the CLIC MBI complex. For the booster linac (bunch charge 0.83 nC), the optimized 18 mm aperture structure with $\Delta = 3$ mm tapering achieves a beam-loading-compensated gradient of 18.47 MV/m, while suppressing integrated transverse wakefields below 10 V/pC/mm/m. The electron injector linac (bunch charge 1.00 nC) reaches 17.67 MV/m with the same structure, satisfying the same wakefield constraint. The positron injector, requiring a larger 22 mm aperture with $\Delta = 2$ mm tapering due to its larger initial emittance and energy spread, achieves a final loaded gradient of 15.41 MV/m with a bunch-to-bunch energy spread of only 0.01%.

The double-train compressed RF pulse scheme enables simultaneous acceleration of electron and positron trains within a single RF pulse, reducing the effective repetition rate from 200 Hz to 100 Hz. This reduction lowers the average RF power demand and thermal load, albeit at the cost of lower peak gradients: 13.52 MV/m for the booster and 12.73 MV/m for the electron injector. The bunch-to-bunch energy spread remains well controlled at approximately 0.1% for both linacs.

These RF performance gains translate directly into substantial hardware and power savings. Compared to the 2012 CDR design [8], which employed 1.5 m structures powered by 50 MW klystrons at 50 Hz, the updated layout (Table 5) reduces the total number of klystrons by 59–67% and the number of accelerating structures by 51–61%, with peak RF power lowered by 34–48%. The table lists the energy gain $\Delta E$, number of klystrons $N_k$, number of RF structures $N_s$, peak RF power $P_\mathrm{peak}$, and average RF power $P_\mathrm{avg}$ for each linac. The e$^+$ injector linac is common to both single-train and double-train configurations. Average RF power decreases by 18% for the double-train scheme despite the doubled repetition rate of 100 Hz, confirming the improved RF efficiency of the new design.

Beyond CLIC, this work supports a unified RF platform for future colliders, leveraging 80 MW klystrons, 3 m structures, and SwissFEL techniques [9], with FCC-ee alignment [10] reducing costs and fostering CERN synergies.

Table 5: Comparison of the Old (CDR, 2012) and New Layouts for the Linacs

| **Linac** | | **2012 Layout** | | | | **New Layout (Single Train)** | | | | **New Layout (Double Train)** | | | |
|---|---|---|---|---|---|---|---|---|---|---|---|---|---|
| | $\Delta E$ **(MeV)** | $N_k$ | $N_s$ | $P_\mathrm{peak}$ (GW) | $P_\mathrm{avg}$ (MW) | $N_k$ | $N_s$ | $P_\mathrm{peak}$ (GW) | $P_\mathrm{avg}$ (MW) | $N_k$ | $N_s$ | $P_\mathrm{peak}$ (GW) | $P_\mathrm{avg}$ (MW) |
| Common Injector | 2660 | 119 | 119 | 5.95 | 2.38 | – | – | – | – | – | – | – | – |
| e$^+$ Drive | 5000 | 112 | 224 | 5.60 | 2.24 | – | – | – | – | – | – | – | – |
| Booster | 6140 | 128 | 256 | 6.40 | 2.56 | 59 | 118 | 4.72 | 4.72 | 79 | 158 | 6.32 | 3.16 |
| e$^-$ Injector | 2660 | – | – | – | – | 27 | 54 | 2.16 | 2.16 | 37 | 74 | 2.96 | 1.48 |
| e$^+$ Injector | 2660 | – | – | – | – | 31 | 62 | 2.48 | 1.24 | 31 | 62 | 2.48 | 1.24 |
| **Total** | - | **359** | **599** | **17.95** | **7.18** | **117** | **234** | **9.36** | **8.12** | **147** | **294** | **11.76** | **5.88** |

## REFERENCES


[1] CLIC Collaboration, "2025 CLIC Readiness Report", https://indico.cern.ch/event/1439855/contributions/6461475/attachments/3045847/5381772/2025_CLIC_Readiness_Report_v2.pdf, Accessed: 26 June 2025, 2025,

[2] A. Kurtulus *et al.*, "Design and optimization of rf structures for the CLIC main beam injector linacs", *Phys. Rev. Accel. Beams*, to be published. doi:10.1103/86pr-nhf7

[3] A. Kurtulus, A. Grudiev, A. Latina, S. Bettoni, P. Craievich, and J.-Y. Raguin, "Rf design and optimization of the high-energy linac for the FCC-ee injector complex", *Phys. Rev. Accel. Beams*, p. 101601, Aug. 2025. doi:10.1103/x2rz-2qxj

[4] A. Grudiev, S. Calatroni, and W. Wuensch, "New local field quantity describing the high gradient limit of accelerating structures", *Phys. Rev. Spec. Top. Accel. Beams*, vol. 12, no. 10, p. 102001, Oct. 2009. doi:10.1103/PhysRevSTAB.12.102001

[5] Z. Farkas, H. Hogg, G. Loew, and P. B. Wilson, "Sled: a method of doubling slac's energy", in *Proc. 9th Int. Conf. on High Energy Accelerators (HEACC'74)*, Stanford, CA, USA, May 1974, pp. 576–583, 1974.

[6] A. Lunin, V. Yakovlev, and A. Grudiev, "Analytical solutions for transient and steady state beam loading in arbitrary traveling wave accelerating structures", *Phys. Rev. Spec. Top. Accel. Beams*, vol. 14, p. 052001, 2011. doi:10.1103/PhysRevSTAB.14.052001

[7] K. L. F. Bane and R. L. Gluckstern, "Transverse wakefield of a detuned x-band accelerator structure", SLAC National Accelerator Laboratory, Menlo Park, CA, USA, Rep. SLAC-PUB-5783, 1992. https://www.slac.stanford.edu/pubs/slacpubs/5750/slac-pub-5783.pdf

[8] M. Aicheler *et al.*, "A multi-TeV linear collider based on CLIC technology: CLIC conceptual design report", CERN, Geneva, Switzerland, Geneva, Rep. CERN-2012-007, 2012. doi:10.5170/CERN-2012-007

[9] J.-Y. Raguin and M. Bopp, "The Swiss FEL C-Band Accelerating Structure: RF Design and Thermal Analysis", in *Proc. LINAC'12*, Tel Aviv, Israel, Sep. 2012, paper TUPB012, pp. 501–503. https://jacow.org/LINAC2012/papers/TUPB012.pdf

[10] M. Benedikt, F. Zimmermann, *et al.*, "Future Circular Collider Feasibility Study Report Volume 2: Accelerators, technical infrastructure and safety", CERN, Geneva, Switzerland, Geneva, Rep. CERN-FCC-ACC-2025-0004, 2025. doi:10.17181/CERN.EBAY.7W4X